ELSEVIER

Journal of Neuroscience Methods 69 (1996) 123–136

JOURNAL OF NEUROSCIENCE METHODS

Review article

Fractal methods and results in cellular morphology – dimensions, lacunarity and multifractals

T.G. Smith, Jr. [a,*], G.D. Lange [b], W.B. Marks [c]

[a] *Laboratory of Neurophysiology, NINDS, National Institutes of Health, Bethesda, MD 20892, USA*
[b] *Instrumentation and Computer Section, NINDS, National Institutes of Health, Bethesda, MD 20892, USA*
[c] *Laboratory of Neural Control, NINDS, National Institutes of Health, Bethesda, MD 20892, USA*

Received 17 October 1995; accepted 18 May 1996

Abstract

This paper discusses the concepts of fractal geometry in a cellular biological context. It defines the concept of the fractal dimension, D, as a measure of complexity and illustrates the two different general ways of quantitatively measuring D by length-related and mass-related methods. Then, these several Ds are compared and contrasted. A goal of the paper is to find methods other than length-related measures that can distinguish between two objects that have the same D but are structurally different. The mass-related D is shown potentially to be such a measure. The concept of lacunarity, L, is defined and methods of measuring L are illustrated. L is also shown to be a potentially distinguishing measure. Finally, the notion of multifracticality is defined and illustrated to exist in certain individual nerve and glial cells.

Keywords: Fractal geometry; Fractal dimension; Lacunarity; Multifractal; Self-similarity; Cell borders

Contents

* Corresponding author. E-mail: tgs@codon.nih.gov

0165-0270/96/$15.00 Published by Elsevier Science B.V.
PII S0165-0270(96)00080-5

1. Introduction

This paper presents a restricted review of the application of fractal geometry to quantitative cellular morphology. In presenting these methods and their associated results we hope to be able to develop a coherent discussion of fractal geometry. Fractals and many natural objects have a number of special properties. First, they are complex as is manifest in their 'roughness'. Second, they may have structural variation or inhomogeneities that may be manifest by 'texture'. The fractal dimension (D) measures the former and the lacunarity (L) measures the latter (Mandelbrot, 1982, 1994). This paper will deal with the conceptual and methodological aspects of fractal geometry concerning these properties.

Fractal geometry can be considered as an extension of conventional (Euclidean) geometry. Conventionally, we consider integer dimensions which are exponents on length, i.e., surface = length^2 or volume = length^3. The exponent is the dimension. Fractal geometry allows for there to be measures which change in a non-integer or fractional way when the unit of measurement changes, hence the term 'fractal'. The governing exponent, D, is called the fractal dimension (Mandelbrot, 1982). If one is interested in globally describing the shapes of objects quantitatively, one can associate D values with complexity of form (Cutting and Garvin, 1987; Smith et al., 1989; Smith and Lange, 1996). Analytic Euclidean geometry does not easily lend itself to this goal, but fractal geometry does. This is largely because complexity of form and scaling are intimately related. For example, to the microscopist, the feature of an object that dictates that more fine structure will be revealed as it is magnified is its morphological complexity (e.g., increased resolution and detail). Fractal objects have this property. It is known as self-similarity or scale invariance. A self-similar object appears qualitatively the same, irrespective of magnification. This suggests that fractal geometry might provide useful measures of this type of complexity. Indeed, the fractal dimension measures the rate of addition of structural detail with increasing magnification, scale or resolution. The fractal dimension, therefore, serves as a quantifier of complexity of form (Cutting and Garvin, 1987). Fractal geometry has proven to be a useful tool in quantifying the structure of a wide range of idealized and naturally occurring objects. The range of application extends from pure and applied mathematics, through physics and chemistry to biology and medicine.

Of course this is but one definition of complexity. To some, complexity could be embodied in a lack of predictability as in complex poetry or music. A true fractal is the antithesis of this. If one knows its form at one resolution, one can exactly predict its form at any other scale.

Those new to fractal geometry may be concerned with the 'meaning' of D. In this context, it should be emphasized that D is a descriptive, quantitative measure; it is a statistic, in the sense that it represents an attempt to estimate a single-valued number for a property (complexity) of an object with a sample of data from the object. Moreover, D does not necessarily imply any underlying mechanism of form generation or function. In general, connections between the empirical values of D and any specific, say, growth mechanisms require the answering of specific scientific questions and not statistical or mathematical ones. One can, for example, view D in much the same way that thermodynamics might view intensive measures such as temperature. That is, as a measure of a property of some object or material, even though in the case of temperature a good deal is known about the underlying mechanisms leading to its value.

As useful as D has been in quantifying structural properties of objects, it is not a unique, sufficient measure. For example, two objects may appear visually very different from one another in their structural characteristics and yet have the same fractal dimension (Smith et al., 1989; Smith and Lange, 1996). In the same sense, two materials' samples may have, say, the same mean value on some measure but be significantly different in some other regards, for instance in their statistical variance. We would hope that we might find other measures which, when taken along with D, constitute sufficient measures of complexity and other global morphological properties. That is, provide a quantitative description of cells that is congruent with our traditional visual impression of complexity. The search for such measures is one goal of this paper.

2. Methods and results

2.1. Methods of calculating fractal dimension

In general, there are two basic approaches to measuring the fractal dimension of an outlined (border) object in a plane. The first, and most commonly used, is length-related and measures the lengths or distances between points on the border of, say, a binary image (i.e., a one-pixel-wide black border on a white background). The resultant D is called the capacity dimension. The second or mass-related method counts border pixels located within discs of various diameter, where the discs are randomly centered on the image border. The resultant D is called the 'sandbox' or the cumulative mass dimension (Feder, 1988; Caserta et al., 1990, 1995). In either case, it is the statistics of the samples as a function of the size of the sampling domains (ruler lengths, disc diameters, etc.) that is the important measure. When a distance measure is applied, the size of a pixel side becomes the unit of length. When a pixel counting measure is applied, the individual border pixel becomes the unit of mass.

2.2. Length methods

There are several ways of measuring length-related fractal dimensions, which have been detailed elsewhere

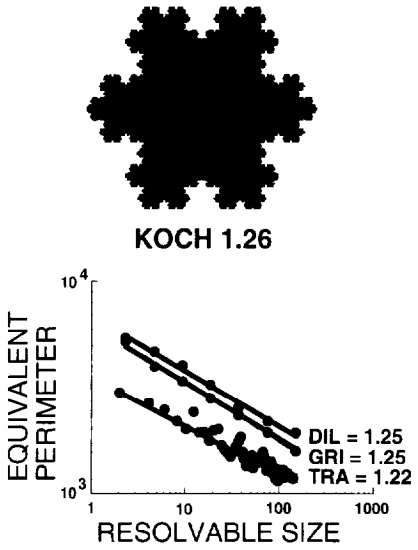

Fig. 1. Measuring the length-related, capacity fractal dimension (D) of a Koch snowflake (A, upper), with a calculated $D = 1.26$ by the dilation (DIL), box counting (GRID) and perimeter trace (TRA) methods. (B, lower) Log-log plots of the equivalent perimeters with measuring elements (resolvable size) from size 2 to 128 pixels, in powers of 2. In this and all log-log plots, the curve fits are a power function. See text.

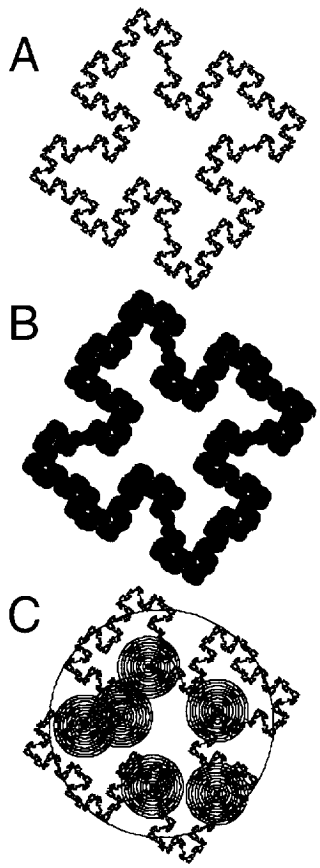

Fig. 2. Examples of length and mass methods results. (A) Image of Koch ($D = 1.50$) quadic island. (B) Length (dilation) method example. Island after dilation with a disc kernel diameter of 16 pixels. Note loss of border detail shown in A. (C) Mass method example. Application of six groups of concentric discs, with various diameters and centered on border of Koch island, all centers lying within the radius of gyration (large circle). See text.

(Smith et al., 1989) and shall only be reviewed here. They can be tested by using the borders of fractals of known D, for example the Koch figures, e.g., in Fig. 1 (Smith et al., 1989) [1]. The classical method of Richardson (Mandelbrot, 1982) involves measuring the perimeter of an object with various lengths of rulers (spans or calipers) (trace method). When the log of the perimeter is plotted against the log of the ruler lengths, a fractal object gives a straight line with a negative slope S. Then, $D = 1 - S$.

A second method is based on the concept of 'covering' the border and is called a 'box counting' or grid method. Here, sets of square boxes (i.e., grids) are used to cover the border. Each set is characterized by a box size. The number of boxes necessary to cover the border is noted as a function of the box size. The log of the number of covering boxes of each size times the length of a box edge is plotted against the log of the length of a box edge. Again, a straight line results, with slope S, and D is calculated as before [2].

A third method, developed by Flook (Flook, 1978; Smith et al., 1989), is called the dilation method. Dilation, in this case, means a widening and smoothing of the border (see Fig. 2B). It can be accomplished by convolution operation with a binary disk, i.e. all the non-zero components of all the convolution kernels have a (Boolean) unitary value. The result is a thickened, but grey scale border. To return this border to Boolean one values, all non-zero pixels are thresholded to a Boolean one. The rate at which the total surface area of the border grows as a function of the diameter of the convolution kernel depends on D. The log of each resulting area divided by the kernel diameter is plotted against the log of the kernel diameter. Yet again, a straight line results with a negative slope S and D is calculated as above.

It should be noted that with length-related methods, the magnitude of the resultant measure (perimeters, etc) increases as the measuring element (ruler, etc.) decreases in size. In a deterministic or mathematical fractal, the increase continues without limit as the measuring element approaches zero or infinity. This is an illustration of the important and defining property of fractals, viz. self-similarity (scaling symmetry or invariance) (Mandelbrot, 1982). Universal self-similarity exists only in mathematical for-

[1] Most images in this paper are shown mainly as silhouettes, for visual clarity. All measurements, however, were done on one-pixel-wide, border-only images.

[2] An old version of NIHImage imaging software program, called ImageFractal and run on Macintosh II computers, performs a box-counting routine on one-pixel wide, binary image files. It is available via FTP from zippy.nimh.nih.gov/pub/NIHImage/spinoffs. The results can be saved as a text file for analysis with any application capable of curve fitting and simple spread sheet manipulations.

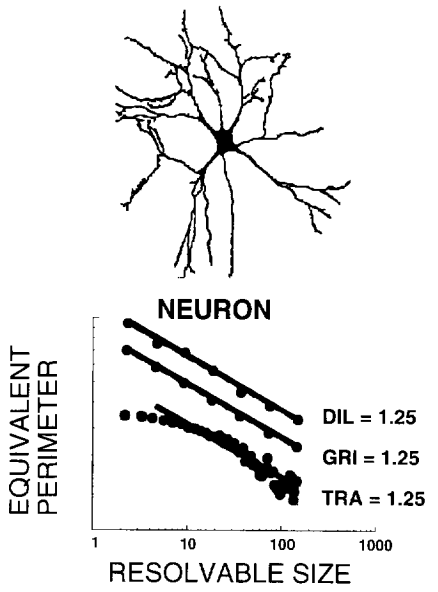

Fig. 3. Measuring the fractal dimension (D) of a cell cultured spinal cord neuron (above) by the dilation (DIL), grid (GRID) and perimeter trace (TRA) methods. (Lower) Log-log plots of the equivalent perimeters with measuring elements (resolvable size) from size 2 to 128 pixels, in powers of 2. See text.

mulas or in computer algorithms. Real world or natural fractals are only self-similar in a statistical sense and have fractal dimensions restricted to ranges of scales (Baumann et al., 1993). That means that the fractal is statistically self-similar and looks qualitatively the same over many scales.

The operations designed to estimate length-related fractal dimensions have a low pass filter character to them. That is, with increases in the size of the measuring elements, the higher spatial frequencies (border roughness) of an image are progressively removed, while leaving the lower spatial frequencies (long branches). This is illustrated for dilation in Fig. 2B. The final D value calculated is an average property of the whole object and has no spatial locality. All three of the methods employed to calculate D are essentially plots of log length vs. log length. Thus, the relevant power relationship is:

$$L(e) = Fe^{S} \quad (1)$$

$L(e)$ is the equivalent perimeter as a function of the resolving element, e, F is a prefactor and S is the slope of the plot of log $L(e)$ vs. log e. Since S is negative and $|S|$ is less than one, D is between 1 and 2 for objects in a plane.

Given sufficient detail and magnification of a cell's binary border, the results of all three operations give similar Ds (see Fig. 3) (Smith et al., 1989) All of these methods consistently underestimate the values of 'true' or deterministic fractals by a few percent (Fig. 1). This is a consequence of the fact that a finite, digitized image with a limited number of pixels (resolution) and cannot realize the detail implicit in a deterministic fractal. This error is probably found in the measurements of natural fractals as well, but since it is a consistent and not random one, and since most results are used comparatively, the error should not significantly affect the conclusions drawn.

The first two methods can readily be implemented on a computer or can even be done (tediously) by hand. The Dilation method is more difficult to program on a computer [3], but is somewhat superior to the others in that it is less sensitive to the location of the image in a frame or to pixelization effects. For example, if the border is not centered in the image frame and does not adequately fill the frame, the grid method will give too few points with large grids and erroneously increase the slopes in the log-log plots. In addition, since many borders become straight (Euclidian) lines with small rulers in perimeter measurements, the slope tends towards zero ($D = 1$) and leads to nonlinearities in the log-log plots (see Fig. 3, TRA). The dilation method is superior because it measures at every point on the border at all scales and hence generates more data (Smith et al., 1989, 1991). In Fig. 4 and all subsequent figures the length-related Ds are from the dilation method.

2.3. Mass method

The mass-oriented measure of D involves counting of border pixels contained in a sampling region (e.g., disc diameters), as a function of the sizes of the sampling regions (Feder, 1988; Caserta et al., 1990, 1995; Smith and Lange, 1996). Here, one centers boxes or circles (the result will be the same irrespective of the shape used) of different sizes at many randomly located points on the border and counts the number of border pixels contained within each box or circle (or disc). This so-called 'sandbox' or cumulative-mass method (Caserta et al., 1995; Smith and Lange, 1996) is a variant of the box-counting method. This is diagramed in Fig. 2C. Then, the log of the number of pixels within each box or circle is plotted against the log of the measuring element (edge size, diameter). A fractal object gives a line with a positive slope, which is the D for that object. The power relationship plotted is:

$$\mu(r) = Ar^{D} \quad (2)$$

where $\mu(r)$ is the number of pixels (mass) in a box of size r, r is the circle diameter or box-edge length, A is a prefactor and D is the slope of the plot of log $\mu(r)$ vs. log r and D is the mass fractal dimension.

The motivation for employing mass measures of fractal objects is several fold. In the first instance, they provide

[3] There is a program macro (Fractal Dilation) for recent versions of the image processing program NIHImage (version 1.53 or later) for the Macintosh that performs the Dilation algorithm on one-pixel wide, binary image files. All the software is available via FTP from zippy.nimh.nih.gov/pub/NIHImage/User Macros. The results can be saved as a text file for analysis with any application capable of curve fitting and simple spread sheet manipulations.

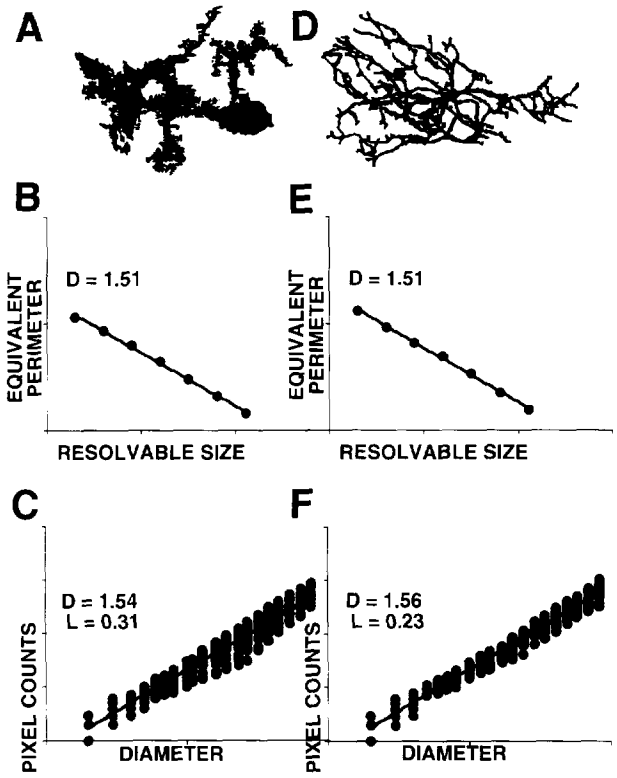

Fig. 4. Two cell cultured neurons (A,D) with the same length-related D (1.51) but with different morphologies. In this and all subsequent figures, length-related Ds were determined by the dilation method. (A) Cerebellar Purkinje cell. (D) Spinal cord cell. (B,E) Log-log plots of equivalent perimeters vs. resolvable size, of A and D, respectively, to give length-related Ds of 1.51. (C,F) Log-log plots of pixel counts as a function of disk diameters, from A and D, to give mass-related Ds of 1.54 and 1.56 and lacunarities (L) of 0.31 and 0.23, respectively.

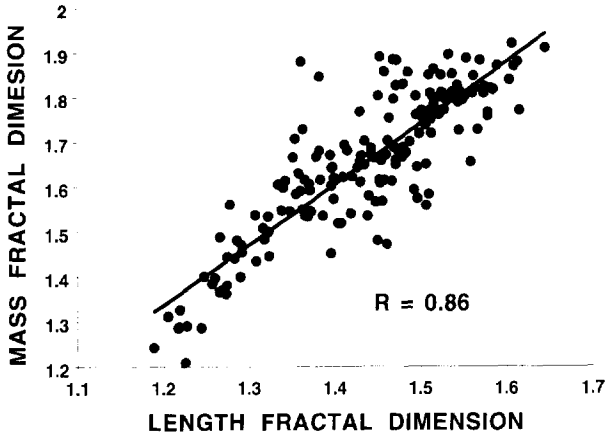

Fig. 5. Linear, pair-wise plot of mass-derived Ds (D-mass) vs. length-derived Ds (D-length) for a variety of cell types. Correlation coefficient = 0.86.

another and often different value(s) of D for the same object analyzed with length measures. For example, for Euclidian objects (lines, squares, etc.) and deterministic fractals, the length and mass fractal D values are theoretically the same. In practice, however, they may differ slightly, due to the less than perfect resolution realized in the finite, digitized images employed, as mentioned above. With natural fractals the two Ds are often different, with the mass fractal D value (usually) being the larger (Fig. 4, cf. B,E and C,F). While, in a statistical sense, the two measures are not completely independent (see Fig. 5), they may still provide useful distinctions in certain cases (Fig. 4; see below). Secondly, and more important, the mass measures provide more information about the fractal object or set than the length measures (Feder, 1988). This can be appreciated from a consideration of conventional box counting (grid) methods. With the length measure, the only concern is the number of boxes of each size required to cover the set (border). This result is a crude measure in that it says nothing about the structure or distribution of pixels within an image (Feder, 1988). Mass measures, however, deal with this distribution property in that the number of pixels in a given size box is the (weighted) measure and thus leads to the notion of mass density (i.e., mass/area). Mass measures also lead conveniently to the concepts of lacunarity and multifractals, as shall be discussed below.

It is instructive to examine the length and mass methods of determining D when applied to Euclidian objects such as lines and circles. Fig. 6 illustrates such results. With a line (Fig. 6A, line), the length plot results in a slope of

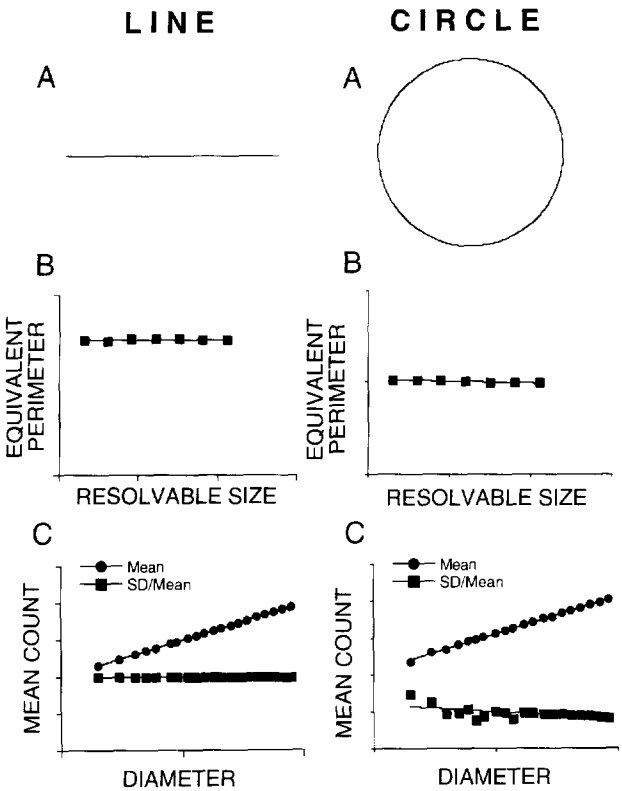

Fig. 6. Euclidian figures: (A) line and circle. Application of length measures (B) and mass measures (C). In C, both mean count and standardized variance or coefficient of variation (standard deviation/mean) are plotted vs. disc diameter. See text.

zero and $D = 1$, as expected (Fig. 6B, line). Likewise, the line mass measure has the expected slope of one and $D = 1$ (Fig. 6C, line), with a constant normalized variance or coefficient of variation (standard deviation/mean). This is a consequence of the fact that all the pixels lie on a single line with constant separation and with constant, zero angle between them. With a circle (Fig. 6A, circle), the length plot gives a slope of almost zero ($S = -0.02$) and a D near one ($D = 1.02$) (Fig. 6B, circle). The mass method also gives a D near one ($D = 1.02$), but the variance is not constant (Fig. 6C, circle), particularly for small diameter discs. This results from the fact that the digitized 'circle' does not have pixels that are all equally spaced along the border, nor have a constant angle between them. The result is, therefore, an artifact of the digitized approximation of a circle and differs slightly from the expected result of $D = 1$ and gives a notion of the limits of accuracy of these measuring methods. One can also see evidence of such artifacts when measures are applied to non-Euclidian, fractal objects.

While natural fractal objects can illustrate the problem of disparate images having the same capacity fractal dimension (Fig. 4), it can be more clearly and convincingly demonstrated with deterministic images that are generated according to some mathematical formula or algorithm, such as the Lindenmayer or L-system method (Prusinkiewicz and Lindenmayer, 1990). Such results are shown in Figs. 7 and 8 for objects of relatively low D (Fig. 7, $D = 1.26$) and relatively high D (Fig. 8, $D = 1.62$), respectively. Note that the objects (A and B) look quite different, but the respective slopes of the length related plots (C and D) are identical. This phenomenon, therefore, may be found throughout the range of borders in a plane of D from 1 to 2.

Natural fractals, however, rarely show such sharp dichotomies of border roughness or profuse branching in isolation. Rather, they represent some (usually unknown) combination of these two properties. It would be useful to be able to sort them out in individual cases, but thus far, however, this has not been practicable (see Section 3).

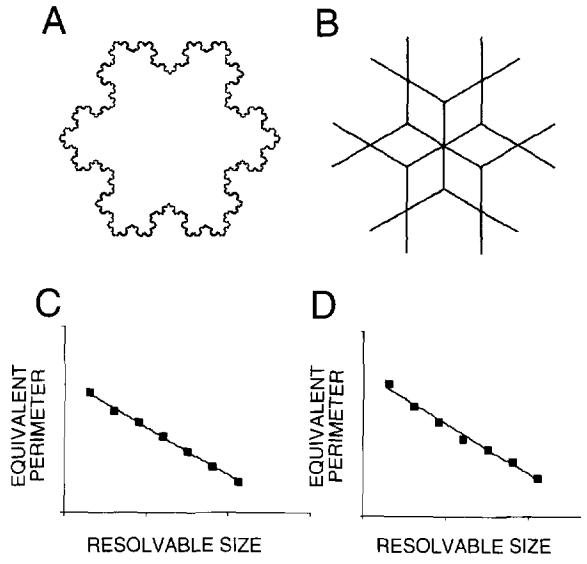

Fig. 7. Koch (A) and L-system-derived images, which look very different, but have the same low valued capacity Ds (1.26). See text.

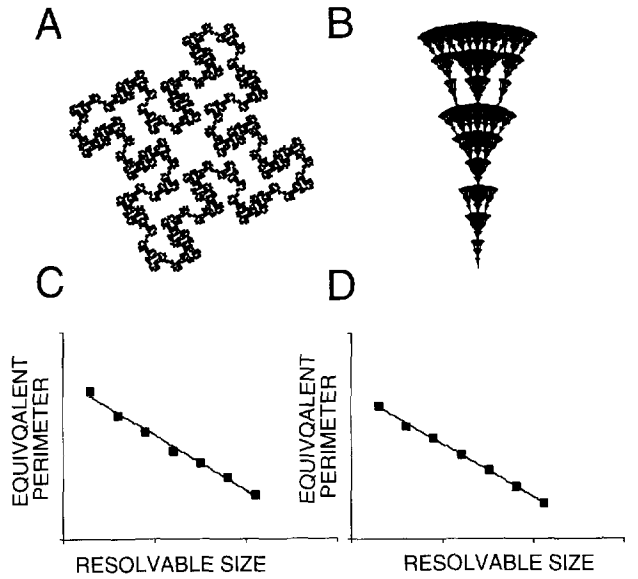

Fig. 8. Koch (A) and L-system-derived images, which look very different, but have same high valued capacity Ds (1.62). See text.

In addition, there is another distinguishing property of fractal objects, which is found in natural fractals, that can also be more clearly demonstrated with stylized images (Fig. 9). This involves images that have either uniformly distributed pixels (Fig. 9, uniform) or non-uniformly distributed pixels (Fig. 9, nonuniform). Here, the global length-derived Ds may be the same (Fig. 9B,E, $D = 1.67$), but the mass-derived ones are both larger and may be unequal (Fig. 9C, $D = 1.90$; F, $D = 1.81$). More importantly, however, is the significant difference in the variances of the two image types. This is indicated by the fact that the vertical scatter of points in the mass measures is smaller in the uniform image (Fig. 9C) than in the nonuniform one (Fig. 9F). The individual points in the vertical scatter at each disc size represent the individual border-located, disc centers. These phenomena relate to lacunarity and to the multifractal character of natural, nonuniform fractal sets (images), which are discussed below.

2.4. Other fractal measures

The preceding text and data represent examples of the focus and attention found in the early history of analytical fractal geometry, particularly as they applied to natural (and especially biological) objects. There, the emphasis was on the search and application of measures of fractal objects such as the capacity D. The attempt was to focus on natural fractal objects that were similar to deterministic fractals in the properties of uniformity of structure and

range of self-similarity. Eventually, it became apparent that many natural fractal objects were often not very structurally uniform and had restricted, and often variable, ranges of self-similarity. Attention was therefore drawn to the variation in structure within fractal objects and a search for different measures to quantitate this variability (see Feder, 1988; Vicsek, 1988). An example, as mentioned, was the observation that a given value of D does not uniquely specify a cellular morphology and very differently looking objects can have the same or very similar Ds (see Fig. 4; see also Figs. 6–9 and 12, for other examples) (Smith et al., 1989). This is a general problem in fractal geometry (Evertz and Mandelbrot, 1992), which can appear in several guises, and falls under the mantel of 'differences in texture' (Mandelbrot, 1994). What is needed, therefore, is at least one other measure that distinguishes such objects. That measure would provide a new quantitative measure and expand the scope of analyzing natural objects.

2.5. Lacunarity

Lacunarity is potentially such measure. Lacunarity can be variously defined and characterized. In a restrictive sense, it is a measure of the lack of rotational or translational invariance (or radial symmetry) in an image (Allain and Cloitre, 1991). The name lacunarity is from the Latin *lacuna* for lack, gap or hole (Mandelbrot, 1982). Hence, a fractal is said to be lacunar if the gaps in an object are wide, i.e., if they have large intervals, holes or voids. But that does not grasp the totality of the lacunarity concept. Indeed, the notions of 'gappiness' may deflect attention away from the essential properties of the measure sought. In a more general sense, lacunarity is a measure of the

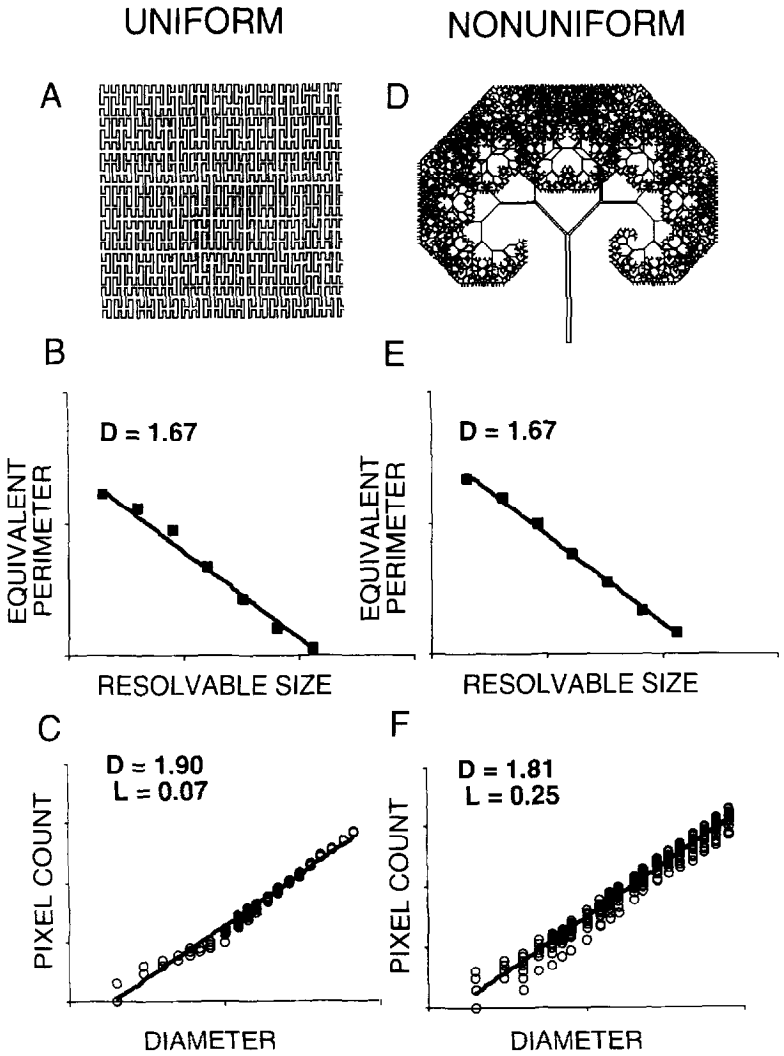

Fig. 9. Peano curve (A, uniform) and L-system tree (D, nonuniform) images. (B,E) Both curves have the same length-derived Ds (1.67), but different mass-derived Ds (C, $D = 1.90$; F, $D = 1.81$; and lacunarities; $L = 0.07$ and 0.25). Note increased vertical spread of points in F as compared to C. See text.

non-uniformity (heterogeneity) of structure or the degree of structural variance within an object. Lacunarity is usually defined in terms of mass related distributions. Thus, high lacunarity is suggested if the vertical scatter of mass-related points around each disc size is large in the log-log plots (see Fig. 4C, F, Fig. 9F Fig. 12C, F).

Mandelbrot (1982) suggests that the magnitude of the prefactor (e.g., A in Eq. (2)) is roughly inversely related to lacunarity. He notes, however, that this definition has limited validity and application. There have been a number of methods proposed for calculating the lacunarity (L) of images in a plane; however, there is no general agreement as to the 'best' or 'correct' procedure (Allain and Cloitre, 1991). Mandelbrot (1982, 1994) has said the lacunarity information is to be found in the variations in fractal measures, which grasps the essence of lacunarity, and most proposed methods focus on this variability. Apparently, all have their limitations and problems, particularly with respect to universality, but they generally provide a measure of the basic properties of L, namely, variability, inhomogeneity, heterogeneity, etc. (Allain and Cloitre, 1991).

A common procedure is to calculate the mean and variance (or standard deviation) of some measure, e.g., the mass (number of pixels) in a box of a given size. For fractals, the result of this calculation is a strong function of scale, thus, to obtain a single number, L, the variance calculations must be normalized. This can be done, for example, by dividing the variance by the square of the mean at each scale (Mandelbrot, 1982). Alternately, one can divide the standard deviation by the mean at each scale to give what, in statistics is called the coefficient of variation or relative dispersion (Bassingthwaighte et al., 1994). Since the former result is simply the square of the latter, either procedure is valid as both increase with increased measured lacunarity, which is the desired result. In this paper, lacunarity will be defined as related to the coefficient of variation. Specifically, L is the average of the coefficient over all scales (box or disc sizes).

For a self-similar object, the coefficient of variation should be constant with scale, since the form of the object at large scales is a magnified version of its form at small scales. That is, the object looks the same at all scales. Therefore, the mean and standard deviation would scale up in the same proportion and their ratio would be a constant, viz., L. Furthermore, the variability of the mass measure about its average value would have a constant vertical scatter when plotted in the log-log graphs, as is approximately the case in Fig. 4C, F, Fig. 9F and Fig. 12C, F.

In this context, the fractal lacunarity of a group of selected images is illustrated in Fig. 10. The L of each image is joined by a vertical line to its L value on the one-dimensional L-axis. The images are identified by their lettered labels and their mass D and L values are shown in Table 1. A few points are worth noting. First, image variation and non-homogeneity increase with increasing L. Second, voids or 'gappiness' in the images show little or no relationship to L, with large gaps appear in images at low L (C, D) and at high L (I, J). Some of the results confirm expectation. For example, the line (A) has a D of one and an L of zero, since it is both Euclidian and has no variability. Others, do not. The digitized circle (C) does not have the expected D of one and L of zero. As in Fig. 6, D is near one, but the variability results from the fact that the digitized circle has elements of straight lines at the top, bottom and sides of the image and of variously sized steps in the other pixel locations around the circle. This

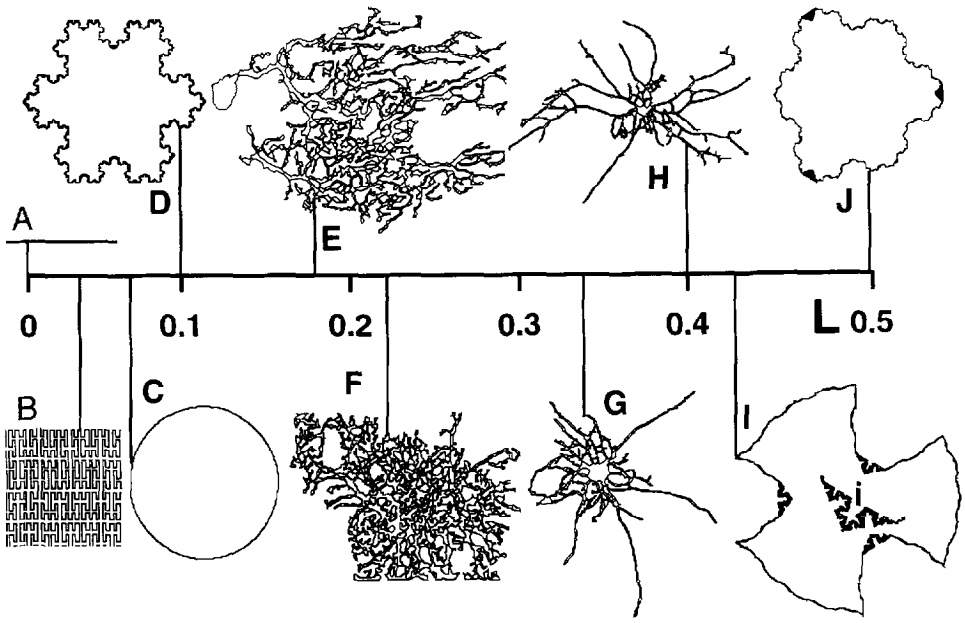

Fig. 10. Illustration of images (A–J) with their lacunarity (L) values joined from the image with a straight line to the one dimension L scale. Inset (i) in image I shows detail of complex region at high magnification.

Table 1
Identification of images shown in Fig. 10, along with their mass fractal dimensions (D) and lacunarity (L) values

Item	D	L
A. Line	1.00	0.00
B. Peano curve	1.90	0.04
C. Circle	1.02	0.07
D. Koch snowflake	1.26	0.10
E. Purkinje neuron	1.89	0.18
F. Brain astrocyte	1.68	0.22
G. Spinal cord neuron no. 1	1.73	0.37
H. Spinal cord neuron no. 2	1.62	0.40
I. L-systems image no. 1	1.32	0.42
J. L-systems image no. 2	1.14	0.49

means that the pixel counts will vary as the discs (Fig. 2C) are located at different points on the circle. Note that the homogeneous, deterministic fractals (B,D) have an L near zero. They should be exactly zero, since they have uniform textures. The discrepancy, again, is due to lack of resolution and pixelization errors of the digitized images. Finally, the largest Ls are found in those L-system derived images that have the greatest separation of D values within the image, as shown in I and J. This suggests an interrelationship with lacunarity and multifractal processes (see Section 3). Since some resolution of the images are lost in their compression for inclusion in the figure, an enlarged segment of the most complex part of an image is shown in image I, inset (i).

What follows is an attempt to measure the lacunarity of a collection of biological cells that has been reported in preliminary form elsewhere (Smith and Lange, 1996). Measurements were made on a cell-by-cell basis. The mass Ds and L were calculated for each cell. When the entire population cells' Ls vs. their mass Ds were plotted, it was found that there was negative correlation of 0.75 between the two measures (see Fig. 11). This suggests (1) that the high D cells, like those near $D = 2$, are sufficiently filling the frame so there is little room for holes or variation and (2) that the two measures are not completely statistically independent (orthogonal) over the entire population. On the other hand, when considered for particular cell pairs

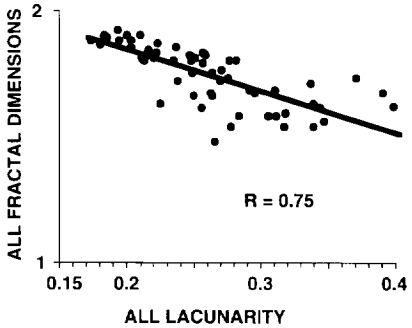

Fig. 11. Pair-wise plot of mass-derived Ds vs. lacunarity of each cell for a number of different cell types. Correlation coefficient = 0.75. See text.

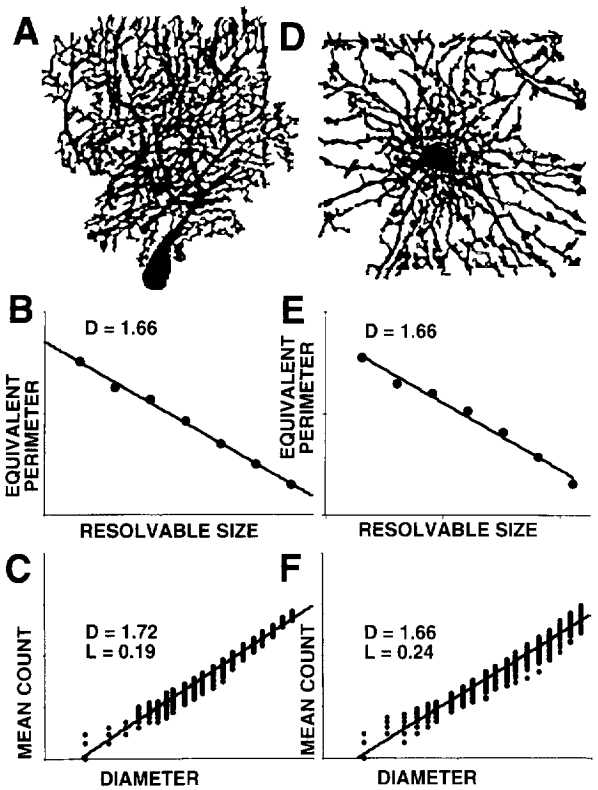

Fig. 12. Two morphologically distinct cell types (A) In-vivo cerebellar Purkinje cell (camera lucida drawing) and (D) cell cultured glial cell), with identical length-related Ds (1.66; in B and E); but different mass dimensions (1.72 and 1.66 and lacunarities (0.19 and 0.24, in C and F).

with identical Ds, the degree of independence may be adequate for fractal lacunarity to provide a useful distinguishing measure (Figs. 4, 9 and 12).

2.6. Multifractal measures

The term multifractal describes (often natural) objects that are neither universally nor statistically self-similar but possess an uneven distribution of complexity within the domain of the object or set. Namely, D varies from point to point within the object. The underlying notion has been alluded to above, as, for example, in the small variance range found in deterministic objects (Fig. 6C, line and circle and Fig. 9C) as opposed to the larger variance found in natural-looking fractals (Figs. 4 and 9F and Fig. 12). The idea can be made more explicit from data obtained by mass measures (cf. Fig. 2C). For example, instead of plotting the global distribution of pixel counts across all the range of border-centered disc locations vs. diameter (Figs. 4, 9 and 12C,F), one plots separately the pixel counts for each individual box-center location vs. diameter (Fig. 13A, peano and tree). Here, a range of straight lines, and hence slopes and Ds, are obtained. From such results histograms of the distributions of D values can be obtained (Fig. 13B, peano and tree). For uniform fractals (Fig. 13B, peano) the range of D values is quite small,

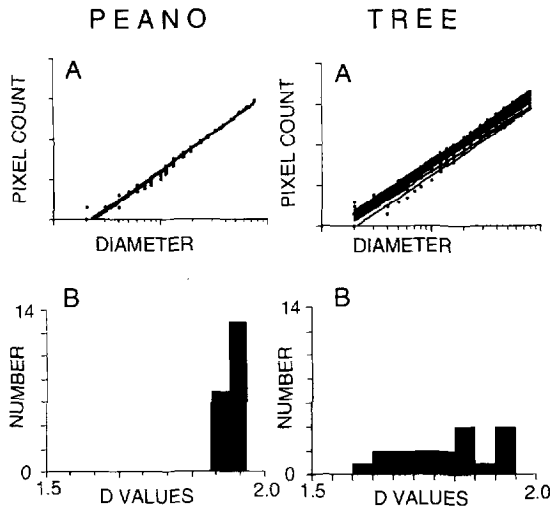

Fig. 13. Log-log plots of pixel counts vs. diameters for each border-centered disc (cf. Fig. 2C) of uniform (PEANO, A) and Nonuniform (TREE, A) images in Fig. 9. (B) Histograms of distribution of Ds for each type. Note that the width of the distribution of peano D values is much less than that of tree. See text.

while with nonuniform, natural-looking (Fig. 13B, tree) fractals, the range is considerably greater. (With deterministic objects, the variance should be zero, but, again, the artifacts of dealing with finite, digitized images introduces a small range of Ds, particularly with small diameter discs (Fig. 9C and Fig. 13B, peano.)) But the larger range of D values for the tree indicate that it is, by definition, multifractal, since the range greatly exceeds any artifactual variation. As yet, however, there are no recognized rules for deciding when the multifractal threshold has been reached in any real life situation.

Fig. 14 shows a similar analysis for the cells shown in Figs. 4 and 12. Their histograms also show a considerably greater variation than is likely from artifacts alone and suggest that these cells have a multifractal structure (cf. Fig. 14 with Fig. 13B, peano). To our knowledge this is the first demonstration of multifractal properties in biological structures.

2.7. Silhouettes or borders?

Finally, there is some divergence in the literature as to the 'proper' or 'correct' objects for applying fractal analysis, namely, should it be an object's silhouette or its border? We have argued (Smith and Lange, 1996) that in a fractal analysis of cellular shape, it is the dimension of the border that is of interest and that it alone should be studied (one-pixel-wide, binary (black-on-white, border-only images). Since in our work (e.g., with Golgi stains) the cell interior is often a featureless Euclidian, with integer dimension, measuring silhouettes would give the 'wrong' D,

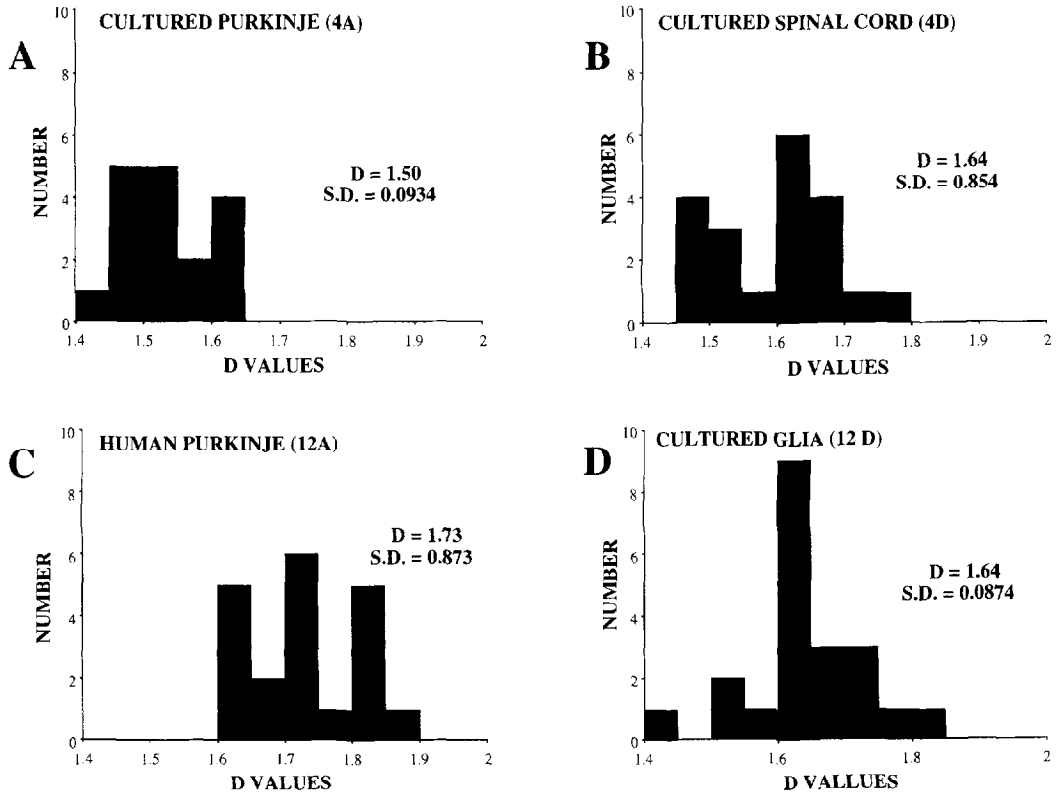

Fig. 14. Histograms of distribution of D values from cells shown in Fig. 4 and Fig. 12. (A) Cultured Purkinje cell (4A). (B) Cultured spinal cord neuron (4D). (C) Human Purkinje cell (12A). (D) Cultured glia cell (12D). Note the wide range of distribution of D values, when compared to uniform fractal (cf. Fig. 13B, PEANO).

namely a mixed D (see Section 3). We have examined the matter by studying objects of known D (lines, squares, Koch figures, etc.). We have used the box-counting algorithm to measure length and the mass radius method for mass, as described in this paper. We begin with one pixel wide objects and progressively increase the width of the object, on the inside, by a known amount. Then, both methods are applied to all objects and the resulting Ds plotted against object width and compared them with images that remained border-only objects. The objects occupied approximately half the width of a plane in a 256×256 pixel frame. All the results showed that as long as the widths were less than about 10 pixels wide, the results of all measurements on both filled and empty borders were essentially the same. With objects whose border widths were greater than about 10 pixels, there was a significant departure in the results from the border-only and the filled border images, with the former maintaining the expected values (of one for lines or boxes) and the latter increasing sigmoidally to a D value of two. The final value of two was reached when the width of the line was near its length and the borders were nearly filled, as expected (results not shown). The conclusion we draw from this experiment is that, since one does not always work with objects that have widths small with respect to their overall size, it is advisable to employ border-only images to obtain the correct result [4].

3. Discussion

From the results and conclusions of previous research reported in this review (see below), it should be abundantly clear that the concepts of fractal geometry and the use of the notion of a fractal dimension are helpful analytical tools for quantitative studies of the morphology of individual biological cells. To the traditional measure of linear-related, capacity fractal dimension, one can now add the newer measures of mass fractal dimension and lacunarity, and the notion of multifractal. While these newer measures may not be completely independent of (orthogonal to) the capacity dimension (Figs. 5 and 11), they both may be able to distinguish, on a case-by-case basis, between objects that appear different, but have the same capacity fractal dimension (Figs. 4, 9 and 12).

[4] Since the acceptance of this paper, a chapter in a book has appeared which contains information that validates this conclusion. Vicsek points out that theoretical fractals in a plane, in addition to having an infinite length, have a zero area. The closest one can come to this in a digitized image is a one-pixel-wide border. For reference see Vicsek, T. Fractal geometry. In: P.M. Iannaccone and M. Kohka (eds), Fractal Geometry in Biological Systems. CRC Press, New York, 1996.

3.1. Factors affecting the fractal dimension

The characteristics of cellular morphology that most influence the magnitude of D are the profuseness of branching and the ruggedness or roughness of the border, with increases in either leading to a larger D (Smith et al., 1989). This means, of course, that two cells that look very different (e.g, one with few branches and a rugged border (Fig. 4A); and the other with a smooth border and many branches (Fig. 4D)) but may have the same D (see Fig. 4B,E). This result emphasizes that, with such global or statistical measures, D provides no unique morphological specification. As an aside one might note that the concepts of border roughness and profuse branching relate to a given image at a particular magnification at a higher magnification a rough border might appear as diffuse branching and, at a lower magnification, profuse branching might look like rough border. These are manifestations of self-similarity.

The exact method employed to measure D does not depend on whether an image is self-similar. That is determined by the log-log plots. The range of the linear slope of those plots identifies the range of self-similarity (Smith et al., 1989; Baumann et al., 1993). In the work considered here, it is only the border that is fractal. The structureless interior is Euclidian, not fractal.

3.2. Fractal experiments in cell morphology

Most of the experiments reported in the literature that apply the concepts of fractal geometry to cellular morphology involve mainly the use of length-related measures of D. This reflects, in part, the historical precedence of these over mass measures. A recent review (Smith and Lange, 1996) has covered the reported results in considerable detail and may be consulted. Suffice it here that the main areas of that review are summarized:

1. Experiments that focus on the quantification and classification of cellular morphology.
   a. Tissue cultured neurons and glial cells (Smith et al., 1989, 1991; Caserta et al., 1990, 1995; Reichenbach et al., 1992; McKinnon et al., 1993).
   b. Retinal ganglion cells (Montague and Friedlander, 1989, 1991; Morigiwa et al., 1989; Caserta et al., 1990, 1995).
   c. Vertebrate CNS motor cortical cells (Porter et al., 1991).
   d. Vertebrate cerebellar glial cells (Siegel et al., 1991; Senitz et al., 1995).
2. Experiments that use the fractal dimension to study cellular growth and differentiation (Smith et al., 1991; Smith and Behar, 1994; Smith and Neale, 1994).
3. Studies that proposed models for cellular growth and differentiation (Pellionisz, 1989; Caserta et al., 1990; Neale et al., 1993; Smith and Neale, 1994; Smith and Lange, 1996).

The results of Fig. 6 raise questions about the usual dichotomy of designating objects 'fractal' and 'non-fractal'. Mandelbrot has pointed out that the distinction between a fractal and a Euclidian is not always clear (Mandelbrot, 1982, 1994; see also Tautu, 1994). In the context of the notion of fractal geometry as an extension of conventional (Euclidian) geometry and of analytical experiments, the distinction appears to be even less clear. For example, the objects usually described as Euclidian or non-fractal (points, lines, circles, cubes, etc.) may be viewed as fractal objects with the lowest complexity (integer fractal dimensions) within their respective dimension domains (zero to one, one to two, etc.)

3.3. Different fractal dimensions

In a recent paper, Caserta et al. (1995) made a quantitative comparison between the length related, box-counting and mass dimension methods of measuring D on retinal ganglion cells. They conclude that the latter is the preferred method because it is more 'accurate'. We find this a curious conclusion, since, we see these two methods as measuring two different aspects of a cell's border. As we have pointed out in some detail in this paper, the former method is a measure of the cell's perimeter, while the latter is a measure of its mass, or perhaps better, it's density. Now it is true that they may both have very nearly the same value of D, they are not usually exactly the same (Figs. 4, 9 and 12) and can provide a measure that can distinguish between cells, one of the 'distinguishing' measures we seek in this paper.

3.4. Multifractals and self-similarity

The finding that objects can be multifractal, namely, that the fractal dimension varies as a function of location within a set (image, frame), potentially raises some fundamental questions about the meaning of a 'fractal object' and 'self-similarity'. Historically the notion of a fractal is that is possesses the property of self-similarity, namely, that a portion of the fractal 'looks' the same as the whole at different scales or magnification. For deterministic, fully developed fractals self-similarity is universal; i.e., that a portion of the border of a fractal is exactly the same as the whole. For natural fractals, the definition of self-similarity was relaxed so that a fractal is only 'statistically' self-similar, i.e., that the portion of the object 'looks' qualitatively like the whole.

The definition of self-similarity has been redefined to focus on a measure related to scale. This has the merit of changing the criterion from a visually, subjective one to one with a mathematical basis. Namely, that an object possesses scale invariance and hence is fractal with a fractal dimension, if the log-log plots of some result (e.g., equivalent mass) vs. log of some measuring element (e.g., box size) produced a 'good' straight line fit over some range of scales. When this range is sufficiently extensive, it is called scale invariance. Again, with deterministic fractals the range is without limit (universal). For natural fractals the requisite range is usually loosely or operationally defined as some order(s) of magnitude of the measuring element range (Baumann et al., 1993). In all practical instances, however, the issue boils down to the question of the 'goodness' of the straight line fit and is usually decided by some statistical criterion (e.g., the correlation coefficient between the data and a straight line model, based on, for example, least-squares criteria).

In many practical situations, the above considerations may seem so small as to border on the inconsequential. But, in the case of multifractals, these issues cannot be avoided. In the case of multifractals, the question arises as to how one is to interpret the global and the local measures of the fractal dimension. To the degree that the global fractal dimension is a statistical measure of the whole object, it represents a measure of its global complexity and, hence, demonstrates the fractal properties of the object as a whole. One the other hand, the local fractal dimensions represents the complexity and the fractal properties of different *loci* within the object. In a sense, this is the essence of multifractals–namely, that objects can have global and different local fractal dimensions and, hence, of difference in complexity. In some cases, the mean D of the multifractal histogram is near the global D. The multifractal concepts extend far wider than the introduction given above, but their general consideration is beyond the scope of this restricted review (see Feder, 1988; Vicsek, 1988; Evertz and Mandelbrot, 1992). Briefly, the consequences of being multifractal are several. The most significant are that multifractals actually possess an infinite number of fractal dimensions and the spectrum of fractal dimensions leads to the definition of quantities that are analogous to the thermodynamic properties of temperature, entropy, etc. (Feder, 1988; Vicsek, 1988)

3.5. Mixed fractals

In their book, Bassingthwaighte et al. (1994) discuss how fractal objects may evolve from single or multiple processes [5]. The first is that a single process, applied at one scale, can spread across all stages and scales to produce a global fractal of singular dimension, namely, a monofractal. This is the conventional concept as to how fractals are produced and is the process involved in generating true fractals. It may begin at a large scale and contract to smaller scales during various stages. This is how, for example, Koch and other fractals are produced by either Mandelbrot's rules (initiator and generator)

[5] By process we mean one mechanism that would lead to a single D, if applied alone and at all stages of object generation (growth) and over all scales.

(Mandelbrot, 1982) or with L-system rules (axiom and production) (Prusinkiewicz and Lindenmayer, 1990). Alternatively, the process may spread from the small to the large scale at all stages, as in diffusion limited aggregation or DLA (Feder, 1988; Vicsek, 1988). Furthermore, this may be how single process natural fractals grow, although it is not easy to verify.

On the other hand, their may be two or more processes operating to produce a fractal with one global D. In principle, this may occur in many ways. For example, there could be the simultaneous global application of the processes at all stages and scales. Or the processes may be locally separate and applied simultaneously at all scales. This latter mechanism is most likely to produce a multifractal. Alternatively, either global or local processes could be applied at different stages and scales; or any combination of the above. In practice, however, it is usually difficult or impossible to know or demonstrate whether any of these mechanisms are operating with deterministic or natural fractals, as has been discussed by Russ (1994).

The preceding discussion allows us to put in context some of the results we and others have made here and elsewhere. First, consider log-log plots where there is no easily determined or extensive range of a straight line. The conventional wisdom is that the object is not a fractal. It may be, however, that the object is a mixed fractal. That is, there a two or more mechanisms involved, where one is apparent at large scales and another at small scales. This is what may be happening in certain neurons that have a steep slope at large scales and a shallow to zero slope at small scales. This is illustrated in Fig. 3, TRA plot, where the Euclidian (straight line) properties dominate at small scales.

In addition, one can mix the production rules of two true fractals in an L-system production (Prusinkiewicz and Lindenmayer, 1990) to produce a mixed fractal (either globally or locally), to obtain either a straight line that has an unknown relationship with the underlying fractals or the absence of any straight line. The resultant object has a fractal appearance, but the plots do not help one to understand how the results were obtained (unpublished observations).

3.6. Lacunarity and multifractals

We mentioned in the result that there may be a relationship between lacunarity and multifractals. Let us discuss what that might be. In the first place, both are measures of variation. And they may both be manifestations of mixed and/or multi-fractals. Lacunarity relates to the variations in the pixel counts at all box sizes (scales) and at all box centers. Thus, it suggests that more than one process is applied at all stages and all scales in fractal object generation. Multifractals, by definition, indicate local variations across the object and probably represent different processes that are applied at different loci and presumably at all stages and scales.

3.7. Fractal design

The notion that biological tree-like, fractal structures represent an optimal design for a particular function is generally accepted. For example, such ideas have been proposed for the lung for the flow of air and the vascular bed for the flow of blood (Bassingthwaighte et al., 1994). It may well be that the fractal, dendritic trees of neurons are also optimally designed, but in this case for the flow of their most important commodity: information (see Smith and Lange (1996) for a discussion). In addition, the fractal dimension is said to be a measure of the number of degrees of freedom involved in the underlying object generation mechanisms (Mayer-Kress, 1985). That neurons have different Ds suggests that some neurons have more degrees of freedom required for their growth and differentiation than others. Moreover, they may change during growth and differentiation with changes in D (Smith and Behar, 1994; Smith and Neale, 1994).

4. Conclusion

We believe that it is clear from the examples in this and other reviews that the use of fractal geometry in microscopic anatomy is now well established. It would seem that calculation of fractal dimensions and other related parameters are useful as quantitative morphological and developmental descriptors. Perhaps the most promising is the possibility that they will be increasingly useful in establishing links between structure and function. And, they may lead to a definition of the rules of growth and differentiation of biological cells, which may be the prerequisite for the delineation of the various basic mechanisms involved in fractal form generation.

References

Allain, C. and Cloitre, M. (1991) Characterizing the lacunarity of randon and deterministic fractal sets. Phys. Rev. A, 44: 3552–3558.

Bassingthwaighte, J.B., Leibovitch, L.S. and West, B.J. (1994) Fractal physiology. American Physiological Society Methods in Physiology Series, Oxford University Press, New York.

Baumann, G., Barth, A. and Nonnenmacher, T.F. (1993) Measuring fractal dimensions of cell contours: Practical approaches and their limitations. In T.F. Nonnemacher, G.A. Losa and E.R. Weible (Eds.), Proceedings of the First International Symposium on Fractals in Biology and Medicine, Birkhäuser-Verlag, Basel, pp. 182–189.

Caserta, F., Eldred, W.D., Fernandez, E., Hausman, R.E., Stanford, L.R., Bulderev, S.V., Schwarzer, S. and Stanley, H.E. (1995) Determination of fractal dimension of physiologically characterized neurons in two and three dimensions. J. Neurosci. Methods, 56: 133–144.

Caserta, F., Stanley, H.E., Eldred, W.D., Dacord, G., Hausman, R.E. and

Nittman, J. (1990) Physical mechanisms underlying neurite outgrowth: A quantitative analysis of neuronal shape, Phys. Rev. Lett., 64: 95–98.

Cutting, J.E. and Garvin, J.J. (1987) Fractal curves and complexity, Percept. Psychophys., 42: 365–370.

Evertz, C.J.G. and Mandelbrot, B.B. (1992) Mulltifractal measures. In H.-O. Peirgen, H. Jürgens and D. Saupe (Eds.), Chaos and Fractals: New Frontiers in Science, Springer-Verlag, New York, pp. 841–881.

Feder, J. (1988) Fractals, Plenum Press, New York.

Flook, A.G. (1978) The use of dilation logic on the quantimet to achieve fractal dimension characterisation of textured and structured profiles, Powder Technol., 21: 295–298.

Mandelbrot, B.B. (1982) The Fractal Geometry of Nature, W.H. Freeman, New York.

Mandelbrot, B.B. (1994) Fractals lacunarity, and how it can be tuned and measured. In T.F. Nonnenmacher, G.A. Losa and E.R. Weibel (Eds.), Fractals in Biology and Medicine, Birkhäuser Verlag, Boston, pp. 21–28.

Mayer-Kress, G. (1985) Introductory remarks. In G. Mayer-Kress (Ed.), Dimensions and Entropies in Chaotic Systems, Springer, New York, pp. 2–5.

McKinnon, R.D., Smith, C., Behar, T., Smith, T.G., Jr. and Dubois-Dalcq, M. (1993) Distinct effects of bFGF and PDGF on oligodendrocyte progenitor cells, Glia, 7: 245–254.

Montague, P.R. and Friedlander, M.J. (1989) Expression of an intrinsic growth strategy by mammalian retinal neurons, Proc. Natl. Acad. Sci. USA, 86: 7223–7227.

Montague, P.R. and Friedlander, M.J. (1991) Morphogenesis and territorial coverage by isolated mammalian retinal ganglion cells, J. Neurosci., 11: 1440-1457.

Morigiwa, K., Tauchi, M. and Fukuka, Y. (1989) Fractal analysis of ganglion cell dendritic branching patterns of the rat and cat reninae, Neurosci. Res. (Suppl.), 10: S131–S140.

Neale, E.A., Bowers, L.M. and Smith, T.G., Jr. (1993) Early dendrite development in spinal cord cell cultures: a quantitative study, J. Neurosci. Res., 34: 54–66.

Pellionisz, A.J. (1989) Neural geometry: Towards a fractal model of neurons. In R.M.J. Coterill (Ed.), Models of Brain Function, Cambridge University Press, Cambridge, pp. 453–464.

Porter, R., Ghosh, S., Lange, G.D. and Smith, T.G., Jr. (1991) A fractal analysis of pyramidal neurons in mammalian motor cortex, Neurosci Lett., 130: 112–116.

Prusinkiewicz, P. and Lindenmayer, A. (1990) The Algorithmic Beauty of Plants, Springer Verlag, New York.

Reichenbach, A., Siegel, A., Senitz, D. and Smith, T.G., Jr. (1992) A comparative fractal analysis of various mammalian astroglial cell types, NeuroImage, 1: 69–77.

Russ, J.C. (1994) Fractal Surfaces. Plenum Press, New York.

Senitz, D., Reichenbach, A. and Smith, T.G., Jr. (1995) Surface complexity of human neocortical astrocytic cells: changes and development, Brain Res. 36: 531–537.

Siegel, A., Reichenbach, A., Hanke, S., Senitz, D., Brauer, K. and Smith, T.G., Jr. (1991) Comparative morphometry of Bergmann glial (Golgi epithelial) cells. A Golgi study, Anat. Embryol., 183: 605–612.

Smith, T.G., Jr. and Behar, T.N. (1994) Comparative fractal analysis of cultured glia derived from optic nerve and brain demonstrate different rates of morphological differentiation, Brain Res., 634: 181–190.

Smith, T.G., Jr., Behar, T.N., Lange, G.D., Marks, W.B. and Sheriff, W.H., Jr. (1991) A fractal analysis of cultured rat optic nerve glial growth and differentiation, Neuroscience, 41: 159–166.

Smith, T.G., Jr. and Lange, G.D. (1996) Fractal studies of neuronal and glial morphology. In P.M. Iannaccone (Ed.), Fractal Geometry in Biological Systems: An Analytical Approach, CRC Press, Boca Raton, FL, pp.173–186

Smith, T.G., Jr., Marks, W.B., Lange, G.D., Sheriff, W.H., Jr. and Neale, E.A. (1989) A fractal analysis of cell images, J. Neurosci. Methods, 27: 173–180.

Smith, T.G., Jr. and Neale, E.A. (1994) Fractal analysis of morphological differentiation of spinal cord neurons in cell culture. In T.F. Nonnenmacher, G.A. Losa and E.R. Weible (Eds.), Proceedings of the First International Symposium on Fractals in Biology and Medicine, Birkhäuser-Verlag, Basel, pp. 210–220.

Tautu, P. (1994) Fractal and non-fractal growth of biological cell systems. In T.F. Nonnenmacher, G.A. Losa and E.R. Weible (Eds.), Proceedings of the First International Symposium on Fractals in Biology and Medicine, Birkhäuser-Verlag, Basel, pp. 86–103.

Vicsek, T. (1988) Fractal Growth Phenomena, World Scientific, Singapore.